Quasiparticle nonequilibrium dynamics in a superconducting Ta film

L. Li, L. Frunzio, C. M. Wilson, and D. E. Prober[a)]
Department of Applied Physics and Department of Physics, Yale University, New Haven, Connecticut 06520-8284

(Received 8 August 2002; accepted 6 November 2002)

Nonequilibrium quasiparticle dynamics in Ta are studied using a superconducting Ta film with an Al tunnel junction connected at each end. The quasiparticle system is driven out of the equilibrium by absorption of an x-ray photon. Millions of quasiparticles, created by each photon, diffuse in the Ta film. When the quasiparticles reach the Al junctions they lose energy by emitting phonons and are trapped in the Al film. By measuring the tunneling current, the number of excess quasiparticles can be calculated. In Ta, the diffusion constant of $8.2\pm0.2\ \mathrm{cm}^2/\mathrm{s}$ and quasiparticle lifetime of $83\pm5\ \mu\mathrm{s}$ at 0.21 K are derived from fitting the measured current pulses, and are compared with theoretical predictions. © *2003 American Institute of Physics.* [DOI: 10.1063/1.1533106]

I. INTRODUCTION

Detectors based on superconducting tunnel junctions (STJs) have been studied in the past decade as nondispersive single-photon spectrometers for photon energies of 1 eV to 10 keV.[1–6] The small superconducting energy gap, approximately one milli electron volts, compared to the electron-hole excitation energy in semiconductors, approximately one electron volt, gives a much larger number of excitations ($\sim10^3$). This improves the energy resolution of the STJ detectors compared to semiconductor detectors. STJ-based detectors also provide timing information and high-quantum efficiency.

This work investigates the nonequilibrium dynamics of the quasiparticles in a Ta film absorber. The understanding is essential for designing and optimizing such detectors and potentially for understanding fundamental nonequilibrium phenomena in *d*-band superconductors. Quasiparticle loss, diffusion rate, and trapping are all studied. We show how they limit the speed of the photon detector's response. We have previously presented results for the x-ray energy resolution for a device with length $L=200\ \mu\mathrm{m}$, and analyzed how that depends on the tunnel junction and ground contact design.[7]

In the devices studied, photons are absorbed in one superconductor Ta and the charge is read out from an Al–AlOx–Al tunnel junction. The 600 nm thick Ta film absorber is contacted by an Al tunnel junction on each end, shown in Fig. 1. Ta is chosen as the x-ray photon absorber because of its higher absorption efficiency and longer quasiparticle lifetime compared to Nb.[8] The device geometry[2,3,9] provides one-dimensional spatial imaging using the division of the quasiparticle charge between the two junctions to determine the location of the photon absorption event. When a photon with energy E is absorbed in the superconducting Ta film, it breaks Cooper pairs and creates an average number $N_o=E/\varepsilon$ of excess quasiparticles ($\varepsilon=1.74\Delta^1$). They diffuse at an energy slightly larger than the Ta gap energy, $\Delta_{\mathrm{Ta}}=700\ \mu\mathrm{eV}$, until they reach an Al trap electrode at one end of the absorber. There they lose energy and scatter down toward the Al gap energy ($\Delta_{\mathrm{Al}}=180\ \mu\mathrm{eV}$) by phonon emission, and are trapped in the Al once the energy is less than Δ_{Ta}. These quasiparticles then tunnel through the Al oxide barrier and produce a current pulse that is recorded. This current pulse is integrated to give the charge collected from each tunnel junction. The ratio of the charges from the two junctions gives the position of the photon absorption. The sum of the two charges gives the photon energy. Previous studies[10,11] have reported the physics of the readout process of the tunnel junctions.

II. MODELS

In the model used in our simulations, the one-dimensional diffusion equation is used to describe the spatial distribution of the quasiparticle density as a function of time, $n(x,t)$ since the quasiparticle mean-free-path $\sim0.1\ \mu\mathrm{m}$ is much smaller than typical device dimensions and the boundaries can be taken to be lossless. Quasiparticles at the absorber-trap interfaces will diffuse into the trap over a characteristic length $L_{\mathrm{trap}}=1\ \mu\mathrm{m}$[12] while they inelastically scatter down below the Ta gap energy. The diffusion equation for the quasiparticles in the Ta absorber is

$$\frac{\partial \boldsymbol{n}(\boldsymbol{x},\boldsymbol{t})}{\partial \boldsymbol{t}}-\boldsymbol{D}\frac{\partial^2 \boldsymbol{n}(\boldsymbol{x},\boldsymbol{t})}{\partial \boldsymbol{x}^2}=-\frac{\boldsymbol{n}(\boldsymbol{x},\boldsymbol{t})}{\tau_{\mathrm{loss}}}, \tag{1}$$

where D is the diffusion constant of Ta film and τ_{loss} is the quasiparticle lifetime in the Ta absorber.

To study the dynamics of the quasiparticles we calculate how the density changes with time, and simulate the tunnel current through the junction to compare with measured current pulses. In the Al junction we can neglect the spatial dependence of the quasiparticle density due to fast diffusion in Al. We follow the quasiparticle distribution inside the Al junction as a function of energy. Inelastic scattering, recombination with thermal quasiparticles and self-recombination, tunneling, and backtunneling processes in both electrodes of each tunnel junction and out diffusion from each counter-electrode are all included in the simulation.[11,12] The out-diffusion process in the Al counter electrode is one in which

a)Electronic mail: daniel.prober@yale.edu

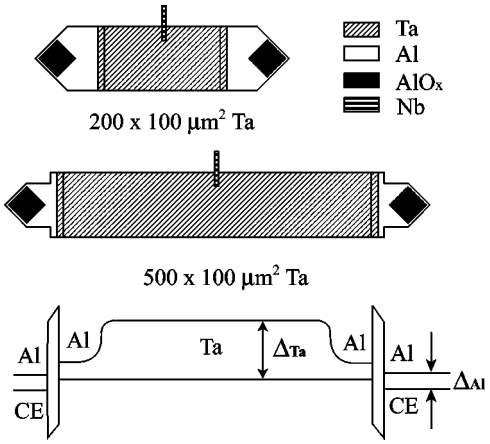

FIG. 1. Geometry of devices Ta1 (top) and Ta2 (center). The black regions are tunnel junctions. The counterelectrodes are not shown. A band diagram is also shown (bottom). In the central region, the Fermi level is constant. The Al counterelectrodes are noted. Device Ta3 has a Ta absorber length $L=1000$ μm but otherwise has the same geometry as device Ta2.

quasiparticles diffuse away from the junction region through the wiring, after which they no longer can tunnel back to the trap electrode. For an out-diffusion time which is short compared to the tunnel time from the counter electrode, a quasiparticle tunnels once and then leaves the region of the tunnel barrier. If the out-diffusion time is long, a quasiparticle can backtunnel from the counterelectrode and return to the trap, and then tunnel again. This process can be repeated, resulting in charge multiplication. We compute the number of quasiparticles crossing the Ta–Al interface, the interface current, and the electrical current crossing the tunnel barrier. It is this tunnel current which causes a current flow in the external circuit. To assign an electrical current to a quasiparticle number current through the Ta–Al interface, we multiply that number current by the electron charge.

Figure 2 shows the simulated interface currents and the tunneling currents from a single photon absorbed near one end of the absorber (at 10 μm distance), or at the center, of a 100 μm long Ta absorber. In the simulation the initial number of quasiparticles in the Al traps is 8 million after trapping multiplication.[12] For this simulation we use the diffusion constant in the Ta as found below in our experiments, 8.2 cm^2/s, and a tunneling time from the trap electrode of 2.5 μs. We assume there is no quasiparticle loss in the Ta and that there is fast out diffusion in the Al counterelectrode after tunneling. This means there is no charge multiplication due to backtunneling. Since the inelastic time in Al is relatively small for an emitted energy $(\Delta_{Ta}-\Delta_{Al})\sim 0.5$ meV, all quasiparticles entering the Al trap from the Ta are trapped. For a photon absorbed near one end, at a distance from one trap of $x_0=10$ μm, diffusion to that trap is fast, $\sim 1/4$ μs, whereas the smaller quasiparticle current entering the more distant trap is much slower; see Fig. 2. For this $L=100$ μm absorber the diffusion times are relatively short, and the dominant slowdown of the tunneling current is the tunnel time of the junction. This is still largely true for an absorption event in the center of the absorber, at $x_0=50$ μm. For this short absorber, the interface current pulse is very short.

We next consider the effect of the absorber length L. For

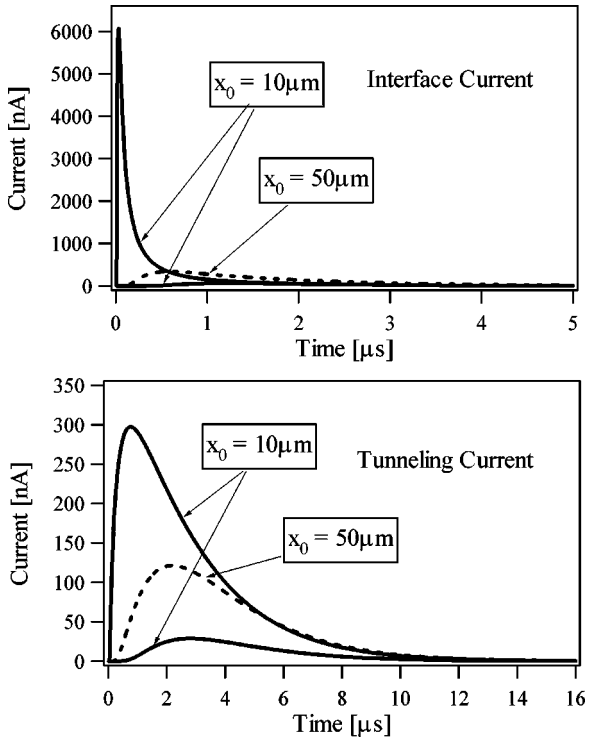

FIG. 2. The top figure shows the simulated interface currents for a photon absorbed at 10 and at 50 μm from one end of a 100 μm long Ta absorber. The two solid curves for $x_0=10$ μm are for the two junctions. The dashed curve for $x_0=50$ μm applies for each of the two junctions. The time scale of the interface current is determined by the diffusion time. For an absorber of a different length, the diffusion time scales as L^2. The bottom figure shows the simulated tunneling current with a tunneling time of 2.5 μs. Note the time scale differs from that of the top figure. The wave form of the tunneling current depends in general on the diffusion time (top figure), the tunneling time, and the out-diffusion time. The quasiparticle loss and the outdiffusion time here are taken to be zero.

photons absorbed at locations 0.1 or 0.5 L and for no quasiparticle loss, the diffusion time and the time scale of the interface current both scale as L^2. The amplitude of the interface current scales inversely with L^2, since the total charge stays the same if there is no quasiparticle loss in the Ta film. The time scale of the tunneling current depends on the diffusion time, the tunneling time, and the out-diffusion time. In Fig. 2, we take the out-diffusion time to be zero. If the Ta absorber is long enough that the diffusion time is much longer than the tunneling time, e.g., for $L=500$ and 1000 μm, the time scale of the tunneling current will depend primarily on the diffusion time. The pulse length of the tunneling current is an important parameter for photon detectors. It sets the maximum count rate of the detector. The longer the absorber, the slower the response time. Thus, the diffusion time sets the limit to the detector size for a given count rate, even with no quasiparticle loss. With quasiparticle loss, the absorber length is further limited.

III. EXPERIMENT

Measurements of tunneling current and integrated charge were done for three devices of different length. These were conducted in a two-stage pumped ^{3}He cryostat at 210 mK. A magnetic field of about 2.5 mT is applied parallel to the

TABLE I. Main parameters of devices studied.

Device	Ta1	Ta2	Ta3
Trap volume [μm^3]	1944	972	972
Absorber length [μm]	200	500	1000
Tunnel time [μs]	6.8	3.4	3.4

substrate, perpendicular to the long dimension of the junctions, to suppress the Josephson current. The device is irradiated with an ^{55}Fe x-ray source which emits MnK$_\alpha$ ($E=5895$ eV) and MnK$_\beta$ ($E=6490$ eV) photons. A low-noise current amplifier is used to measure the current signal from each tunnel junction.[13] The three devices have different absorber lengths, but the same width of 100 μm, and the same junction area, 2025 μm^2. The devices were produced on one passivated Si wafer. The Ta absorber film was dc magnetron sputtered at 750 C in a deposition system with a base pressure of 6×10^{-5} Pa. The Ta film has a residual resistance ratio (RRR)$=17$ with $T_c=4.5$ K. The Josephson current density of each device is 30 A/cm^2. The other main parameters of the three devices are listed in Table I. The tunnel time is computed from the normal state resistance. Their geometries are shown in Fig. 1. Each device is voltage biased at 130 μV.

IV. RESULTS AND DISCUSSIONS

The diffusion constant and quasiparticle lifetime of each device are derived by fitting the current pulses from the two junctions, one at each end of the absorber. Figure 3 shows two experimental pulses, from device Ta2, which are generated by a single x-ray photon, with the fitted pulses. Here we fit an out-diffusion time of 16 μs. Similar pulse fittings also display good agreement for the other two devices. The diffusion constant and the loss parameter $\alpha=L/(D\tau_{\rm loss})^{1/2}$ of quasiparticles in Ta film are the parameters in the model. The determination of the loss parameter is discussed below. The diffusion constant is determined by fitting the experimental plot of the delay time between the two pulses as a function of the peak current, for a number of different current threshold

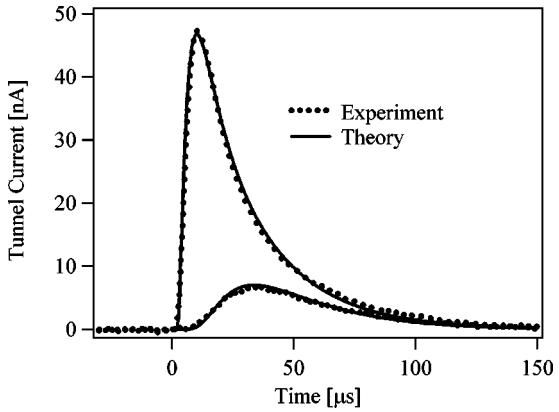

FIG. 3. The dots are the experimental current pulses from the two junctions of device Ta2, for $L=500$ μm, and the solid lines are the fits from the theoretical model.

TABLE II. Diffusion constant and quasiparticle lifetime in the Ta film.

	device Ta1 200 μm	device Ta2 500 μm	device Ta3 1000 μm
$\alpha=L/\sqrt{D\tau_{\rm loss}}$	0.75	1.9	4.0
Diffusion constant D [cm^2/s]	8.2	8.3	8.0
Quasiparticle lifetime $\tau_{\rm loss}$ [μs]	87	83	78

levels. We find a diffusion constant approximately $D=8.2\pm0.2$ cm^2/s for all three devices; see Table II.

The loss parameter α of the quasiparticles in the Ta is determined from the curvature of the plot of Q_1 versus Q_2, where Q_1 and Q_2 are the charges collected by junctions 1 and 2, respectively. $Q_1=\int I_1 dt$ with the integration interval longer than the pulse time. The total charge $Q=Q_1+Q_2$ is proportional to the photon energy E. Figure 4 shows plots of Q_1 versus Q_2 of devices Ta1 and Ta2, and the predicted curves from the model[12] for the Mn K$_\alpha$ x-ray energy. The x-ray events form two traces which correspond to Mn K$_\alpha$ and Mn K$_\beta$ lines with the Mn K$_\alpha$ events about 89% of the total number. In the figure, each dot represents an x-ray photon event. The charge signal was not filtered for this plot, because filtering distorts such a plot, as the current pulses from different absorption locations have different wave

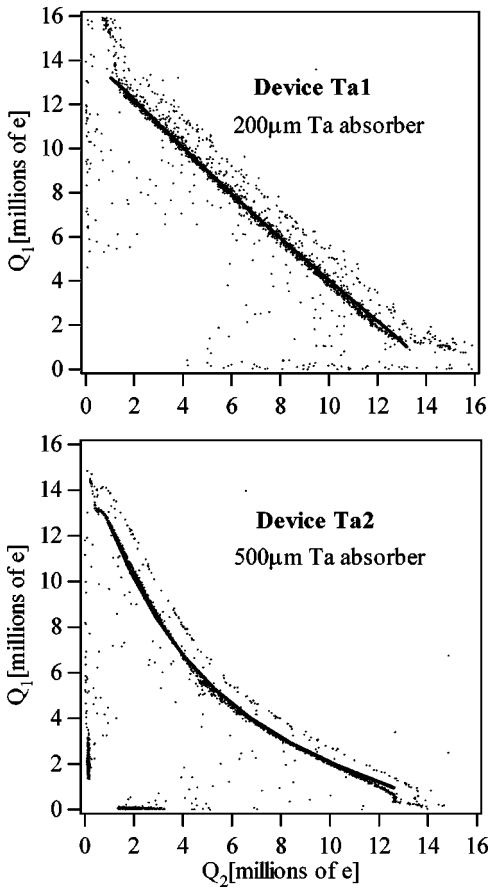

FIG. 4. Q_1 vs Q_2 plots of devices Ta1 and Ta2. The dots are measured individual x-ray events. The lines are from the theoretical model. For Ta1 the fitted line is barely distinguishable from the data.

forms. The energy resolution is determined from plots of filtered charge. If there were no quasiparticle loss in the Ta absorber and no self recombination in the Al trap, a plot of Q_1 versus Q_2 would be a straight line. When there is quasiparticle loss in the absorber, the plot will be curved. The quasiparticles created in the center of the absorber have more loss than those created near the edge, because it takes longer for the quasiparticles in the center to diffuse out from the absorber. The Q_1 versus Q_2 plot of device Ta1 is almost a straight line, which means the quasiparticle loss in the absorber is small. The bending at the two ends is due to absorption events in the 10 μm overlap of Ta and Al. For a longer absorber, it takes longer for the quasiparticles to leave the Ta film. The quasiparticles are more likely to be lost in the Ta. The Q_1 versus Q_2 plot of device Ta2 shows this trend. Device Ta2 is 2.5 times the length of device Ta1. For device Ta2, 30% of the quasiparticles created in the center of the device are lost in the Ta. The quasiparticle loss increases with time. Thus, for device Ta3 with $L=1000$ μm, the measured quasiparticle loss for photons absorbed in the center is about 75%.

The quasiparticle lifetime is calculated from the diffusion constant and the fitted quasiparticle loss parameter α. The results are shown in Table II. To within the experimental accuracy, each parameter is the same in the three devices.

Quasiparticle loss may be caused by spatially uniform loss in the Ta absorber or by loss at the Nb contact in the center, through recombination in Nb oxide regions with a lower-energy gap. The gap in pure Nb is 1.4 meV; Nb oxides can be metallic or low-gap superconductors.[14] The mechanism we have modeled in Fig. 4 is uniform Ta loss. A model in which loss occurs at the Nb contact gives a much different shape. Instead of a smooth curve in the center, as in Fig. 4, Nb loss gives a pointed structure in the center of the Q_1 versus Q_2 plot, and a straight line from the center to each edge. Our data is fit much better by uniform Ta loss. However, we do observe an excess broadening of the energy width ΔE in the center. We have shown that this broadening is caused by the Nb contact.[7] It is caused either by the trapping centers formed by the Nb oxides or by the out diffusion of a small number of quasiparticles through the Nb lead. The dominant mechanism contributing to the energy width at the center of the absorber is loss at the Nb contact. But the dominant loss mechanism in the absorber overall is uniform loss in the Ta film. New designs of the Ta ground contact have eliminated the energy broadening due to the Nb contact.[7]

We now consider the understanding of the parameters we infer from fitting the data. At $T=0.21$ K, the diffusion constant for thermal quasiparticles in Ta is expected to be $D_{\text{Theory}}=D_N(2k_BT/\pi\Delta)^{1/2}=17$ cm^2/s, which is reduced from the normal state value $D_N=1/\rho e^2N(E_F)=130$ cm^2/s by the dispersion relation of the quasiparticles.[15] $N(E_F)$ is the density of electronic states at the Fermi level and $\rho=0.7$ $\mu\Omega$ cm is the film resistivity. When an x-ray photon is absorbed in the Ta, the quasiparticles created by the x-ray photon are under nonequilibrium conditions and have an energy distribution broader than a thermal distribution.[9] The diffusion constant depends on this nonequilibrium quasiparticle energy distribution. Using the simulation of quasiparticle relaxation processes,[9] we predict that the quasiparticles under a nonequilibrium condition should have an effective diffusion constant of $D_{\text{eff}}=27$ cm^2/s. Thus, the measured diffusion constant, $D=8.2$ cm^2/s, is significantly smaller than what we expect. The disagreement is similar to that seen in the previously published data.[16–18] One other group[17] and our group obtained a diffusion constant of 8 cm^2/s. By using a higher-purity epitaxial Ta film, ESA (European Space Agency) researchers achieved a larger diffusion constant of 17 cm^2/s at $T=0.3$ K, which is still three times lower than the theoretical value of 63 cm^2/s.[18,19] The differences between diffusion constants measured by different groups may be caused by the different film structures and qualities. The epitaxial film has faster quasiparticle diffusion than the polycrystalline film because the epitaxial film has fewer crystal grain boundaries for quasiparticle scattering, so the mean free path of quasiparticles in the epitaxial film is longer than that in the polycrystalline film. A similar discrepancy between predicted and measured diffusion constants in polycrystalline Nb films has also been reported.[20,21]

The quasiparticle lifetime we measure is longer than that reported by others.[16–18] The data previously reported by our group[16] was for a short device with $L=200$ μm, produced prior to the devices reported here. That device had $\tau_{\text{loss}}=31$ μs and $D_{\text{Ta}}=8$ cm^2/s. The larger losses may be due to the detailed differences in production of those earlier devices. The parameters reported above for $L=200$ to 1000 μm apply for our present methods of device production. The ESA group[18] obtained $\tau_{\text{loss}}\approx 52$ μs with a 100 nm thick Ta epitaxial film. This difference in τ_{loss} is probably caused by the different film structures and the thickness of the Ta films or by the different substrates.[22] Therefore, the shorter quasiparticle lifetime the ESA group observed may be caused by use of a thinner Ta film with less phonon trapping[22] compared to our Ta film. However, even our measured quasiparticle lifetime of 83 μs is much smaller than the theoretical value of about 1 ms.[23–25] So far, there is no explanation of the shorter lifetimes nor of the slow diffusion constant in Ta. One hypothesis is that the slow diffusion is caused by the small gap variations inside the Ta absorber film at grain boundaries that temporarily trap quasiparticles. There is no full model of this effect, and work remains to understand measured diffusion constants and lifetimes.

V. CONCLUSIONS

In summary, we have successfully modeled the data of three devices with different lengths with self-consistent parameters for the diffusion constant and quasiparticle lifetime. The model is very useful for predicting the performance of UV and optical device designs. At 0.21 K the diffusion constant and quasiparticle lifetime in the Ta film are 8.2 ± 0.2 cm^2/s and 83 ± 5 μs, respectively. These are both smaller than the theoretical values. The quasiparticle diffusion length $\Lambda=(D\tau_{\text{loss}})^{1/2}=260$ μm sets the scale for the length of a Ta film absorber fabricated with our present methods to be less than 1 mm long. The slow diffusion might be improved with further advances in Ta film quality

by using a deposition system with a lower base pressure and a higher-deposition temperature, or a lattice matched substrate.

ACKNOWLEDGMENTS

We thank A. E. Szymkowiak, S. Friedrich, and K. Segall for useful discussions. This research was supported by NASA NAG5-5255 and NASA-GSFC.

[1] N. Booth and D. J. Goldie, Supercond. Sci. Technol. **9**, 493 (1996).
[2] H. Kraus, F. v. Feilitzsch, J. Jochum, R. L. Mossbauer, T. Peterreins, and F. Probst, Phys. Lett. B **321**, 195 (1989).
[3] J. Jochum, H. Krauss, M. Gutsche, B. Kemmather, F. v. Feilitzsch, and R. L. Mossbauer, Ann. Phys. (Leipzig) **2**, 611 (1993).
[4] P. Verhoeve, N. Rando, A. Peacock, A. van Dordrecht, B. G. Taylor, and D. J. Goldie, Appl. Phys. Lett. **72**, 3359 (1998); J. B. le Grand, C. A. Mears, L. J. Hiller, M. Frank, S. E. Labov, H. Netel, D. Chow, S. Friedrich, M. A. Lindeman, and A. T. Barfknecht, *ibid.* **73**, 1295 (1998).
[5] G. Angloher, B. Beckhoff, M. Buhler, F. v. Feilitzsch, T. Hertrich, P. Hettl, J. Hohne, M. Huber, J. Jochum, R. L. Mossbauer, J. Schnagl, F. Scholze and G. Ulm, Nucl. Instrum. Methods Phys. Res. A **444**, 214 (2000); G. Angloher, P. Hettl, M. Huber, J. Jochum, F. v. Feilitzsch and R. L. Mossbauer, J. Appl. Phys. **89**, 1425 (2001).
[6] L. Li, L. Frunzio, C. M. Wilson, K. Segall, D. E. Prober, A. E. Szymkowiak and S. H. Moseley, IEEE Trans. Appl. Supercond. **11**, 685 (2001).
[7] L. Li, L. Frunzio, C. M. Wilson, K. Segall, D. E. Prober, A. E. Szymkowiak, and S. H. Moseley, J. Appl. Phys. **90**, 3645 (2001).
[8] J. B. le Grand, J. Martin, R. P. Huebener, A. W. Hamste, G. C. S. Brons, and J. Flokstra, J. Appl. Phys. **81**, 7413 (1997).
[9] S. Friedrich, Ph.D. thesis, Yale University, 1997.
[10] K. Segall and D. E. Prober, Phys. Rev. B **64**, 1805 (2001).
[11] K. Segall, C. M. Wilson, L. Frunzio, L. Li, S. Friedrich, M. Gaidis, D. E. Prober, A. E. Szymkowiak, and S. H. Moseley, Appl. Phys. Lett. **76**, 3998 (2001).
[12] K. Segall, Ph.D. thesis, Yale University, 2000.
[13] S. Friedrich, K. Segall, M. C. Gaidis, C. M. Wilson, D. E. Prober, P. J. Kindlmann, A. E. Szymkowiak, and S. H. Moseley, IEEE Trans. Appl. Supercond. **7**, 3383 (1997).
[14] J. Halbritter, J. Appl. Phys. **58**, 1320 (1985).
[15] V. Naraynamurti, R. C. Dynes, P. Hu, H. Smith, and W. F. Brinkman, Phys. Rev. B **16**, 6041 (1978).
[16] S. Friedrich, K. Segall, M. C. Gaidis, C. M. Wilson, D. E. Prober, A. E. Szymkowiak, and H. Moseley, Appl. Phys. Lett. **71**, 26 (1997).
[17] Th. Nussbaumer, Ph. Lerch, E. Kirk, A. Zehnder, R. Fuchslin, P. F. Meier, and H. R. Ott, Phys. Rev. B **61**, 9719 (2000).
[18] R. den Hartog, A. Kozorezov, D. Martin, G. Brammertz, P. Verhoeve, A. Peacock, F. Scholze, and D. J. Goldie, *Ninth International Workshop on Low Temperature Detectors*, edited by F. S. Porter, D. McCammon, M. Galeazzi, and C. K. Stahle, AIP Conf. Proc. No. 605 (AIP, Melville, NY, 2002), p. 11.
[19] R. den Hartog, D. Martin, A. Kozorezov, P. Verhoeve, N. Rando, A. Peacock, G. Brammertz, M. Krumrey, D. J. Goldie, and R. Venn, Proc. SPIE **4012**, 237 (2000).
[20] M. L. van den Berg, M. P. Bruijn, J. Gomez, F. B. Kiewiet, P. A. J. de Korte, H. L. van Lieshout, O. J. Luiten, J. Martin, J. B. le Grand, T. Schroeder, and R. P. Huebener, IEEE Trans. Appl. Supercond. **7**, 3363 (1997).
[21] R. Cristiano, E. Esposito, L. Frunzio, C. Nappi, G. Ammendola, L. Parlato, G. Pepe, H. Kraus, and P. Walko, J. Appl. Phys. **86**, 4580 (1999).
[22] K. E. Gray, J. Phys. F: Met. Phys. **1**, 290 (1971).
[23] M. C. Gaidis, Ph.D thesis, Yale University, 1994.
[24] S. B. Kaplan, Low Temp. Phys. **37**, 343 (1979).
[25] S. B. Kaplan, C. C. Chi, D. N. Langenberg, J. J. Chang, S. Jafarey, and D. J. Scalapino, Phys. Rev. B **14**, 4854 (1976).